

# Spin stiffness and resilience phase transition in a noisy toric-rotor code

Morteza Zarei<sup>1,\*</sup> and Mohammad Hossein Zarei<sup>1,†</sup>

<sup>1</sup>*Physics Department, College of Sciences, Shiraz University, Shiraz 71454, Iran*

We use a quantum formalism for the partition function of the classical  $XY$  model to identify a resilience phase transition in a noisy toric-rotor code. Specifically, we consider the toric-rotor code under phase-shift noise described by a von Mises probability distribution and show that the fidelity between the final state after noise and the initial state is proportional to the partition function of the  $XY$  model. We map the temperature of the  $XY$  model to the width of the noise in the toric-rotor code, such that a Kosterlitz–Thouless phase transition at a critical temperature  $T_c$  corresponds to a mixed-state phase transition at a critical width  $\sigma_c$ . To characterize this phase transition, we develop a quantum formalism for the spin stiffness in the  $XY$  model and show that it is mapped to the gate fidelity in the logical subspace of the toric-rotor code. In particular, we introduce a topological order parameter that characterizes the resilience of the toric-rotor code to decoherence within the logical subspace. We show that the logical subspace does not exhibit complete resilience to noise, which is a necessary condition for correctability. However, it exhibits partial resilience to noise for widths less than  $\sigma_c \approx 0.89$ , where the resilience order parameter takes values near 1 and then drops to zero at  $\sigma_c$ . We also use our results to shed light on the correctability of toric-rotor codes in higher dimensions  $d > 2$ . Our work shows that the quantum formalism for partition functions provides a mathematically rigorous framework for studying correctability in continuous-variable quantum codes.

## I. INTRODUCTION

Quantum error-correcting codes are among the best-known approaches for overcoming noise in quantum computation [1–3]. In particular, the interplay between quantum error correction and quantum topological order has attracted significant attention because of the natural robustness of topological phases to local perturbations [4–7]. In topological quantum codes, logical information is stored in a global, topological property of the system in the sense that local errors cannot damage this global information [8, 9]. The toric code is one of the best-known topological codes and has been extensively studied over the past two decades [10–14]. The intrinsic robustness of topological order in the toric code is reflected in its finite error threshold when the system is subjected to a noisy environment [15]. This threshold phenomenon is, in fact, related to a phase transition in the noisy toric code from a correctable to a non-correctable phase [16–18].

Studying phase transition in noisy topological quantum codes has led to the emergence of a new concept of mixed-state topological order [19–21]. While the main focus of traditional studies of error correction is based on the success of decoding algorithms, mixed-state phase transitions provide a new framework for considering correctability based on the intrinsic properties of mixed states describing the noisy quantum codes [22–24]. Since topological properties of these mixed-state phases are not captured by conventional probes of topological order, exploring suitable order parameters has attracted much attention. Consequently, information-theoretic quantities,

such as coherent information and topological entanglement negativity, have been proposed as diagnostic tools [25, 26]. For instance, the error threshold in a noisy toric code can be understood as a decoherence-induced phase transition which is characterized by these information-theoretic quantities [27, 28].

Interestingly, the above studies on noisy topological quantum codes are heavily based on a connection to statistical mechanical models [29, 30]. For example, the error threshold for the toric code is related to the critical point of the ferromagnetic–paramagnetic phase transition in a random-bond Ising model [15, 31]. It is particularly important to root such correspondences in a rigorous mathematical mapping between classical spin models and quantum error-correcting codes. In particular, it is well known that the partition function of classical statistical models can be written as the inner product of a Calderbank-Shor-Steane (CSS) code state and a product state [32, 33]. This quantum formalism was first introduced in the context of measurement-based quantum computation in order to find complete models in statistical mechanics [34, 35]. However, it has also been shown that the above formalism can be used to study phase transitions in noisy topological CSS codes [36]. Using such a mathematical mapping, one can start from an order parameter for a classical phase transition and then find a corresponding order parameter on the quantum side [37, 38].

On the other hand, motivated by platforms based on superconducting circuits [39, 40], rotor- and oscillator-based versions of quantum error-correcting codes has also been proposed [41, 42]. The toric-rotor code is an important example that illustrates significant challenges regarding the error threshold due to the continuity of noise [43, 44]. It is expected that, as in qubit-based codes, the limitations and capabilities of toric-rotor codes can

\* m.zarei@shirazu.ac.ir

† mzare92@shirazu.ac.ir

be determined by mapping to classical statistical models. In this regard, we consider the noisy toric-rotor code in the context of mixed-state topological order to identify a mixed-state phase transition corresponding to the thermal phase transition in the corresponding classical model.

We start our study by developing a quantum formalism for the partition function of the  $XY$  model and showing that it can be mapped to the inner product of a toric-rotor code state and a product state. We then use the above formalism to find the physical correspondence between the  $XY$  model and a noisy toric-rotor code. In particular, we consider a toric-rotor code state in the presence of phase-shift noise described by a von Mises probability distribution [43]. We then show that the fidelity between the noisy mixed state and the initial toric-rotor code state equals the partition function of the  $XY$  model in the sense that temperature on the classical side is mapped to the width of the noise on the quantum side. We conclude that, corresponding to the Kosterlitz-Thouless (KT) phase transition in the  $XY$  model, there is a topological mixed-state phase transition in the noisy toric-rotor code.

In order to characterize the nature of different phases of the noisy toric-rotor code, we identify a suitable order parameter. We consider the spin stiffness, which is nonzero in the KT phase and drops discontinuously to zero in the paramagnetic phase. Then, we use the quantum formalism to map the spin stiffness in the  $XY$  model to a fidelity susceptibility in the noisy toric-rotor code. We find a topological order parameter that has a nonzero value,  $\lambda < 1$ , below a critical noise width  $\sigma_c \approx 0.89$ , vanishes at  $\sigma_c$ , and indicates resilience to noise within the logical code space. Accordingly, we interpret the mixed-state phase transition in the noisy toric-rotor code as a resilience phase transition in the logical subspace of the code. We finally use our results to shed light on the correctability of the toric-rotor code. We show that since the order parameter in the resilient phase is not equal to 1, which is a necessary condition for correctability, the 2D toric-rotor code is not correctable; however, we provide evidence that the code can be correctable in higher dimensions. The structure of the paper is as follows:

In Sec. II, we give a brief introduction to the toric-rotor code. In Sec. III, we introduce our quantum formalism for the partition function of the  $XY$  model. In Sec. IV, we define our noisy model for the toric-rotor code and demonstrate the correspondence between the mixed-state phase transition in the toric-rotor code and the KT phase transition in the  $XY$  model. Finally, in Sec. V, we map the spin stiffness in the  $XY$  model to a resilience order parameter that characterizes the different phases of the model.

## II. TORIC-ROTOR CODE

In this section, we provide a brief introduction to the toric-rotor code. While the toric code is traditionally defined as a many-body system of qubits, the toric-rotor code is obtained by replacing qubits with quantum rotors. The simplest model of a quantum rotor, also known as a  $U(1)$  rotor, is a particle constrained to move along a circular path, such that its position is described by a phase. Another example is a superconducting circuit, in which the phase of the wave function plays a role analogous to the angular position of a particle on a circle [45]. The Hilbert space of the rotor is defined by its canonical variables, including the position variable  $\hat{\theta}$  (or phase), which is continuous and compact, and its conjugate angular-momentum variable  $\hat{\ell}$ , which is discrete and unbounded [42]. The commutation relation associated with these variables is  $[\hat{\theta}, \hat{\ell}] = i$ . This space is described by two orthogonal bases: an angular-position basis  $\{|\theta\rangle \mid \theta \in [0, 2\pi)\}$  and an angular-momentum basis  $\{|\ell\rangle \mid \ell \in \mathbb{Z}\}$ . The connection between these two bases is established by the following relations:

$$|\theta\rangle = \frac{1}{\sqrt{2\pi}} \sum_{\ell \in \mathbb{Z}} e^{-i\ell\theta} |\ell\rangle, \quad |\ell\rangle = \frac{1}{\sqrt{2\pi}} \int_0^{2\pi} d\theta e^{i\ell\theta} |\theta\rangle \quad (1)$$

which are similar to Fourier transformations between position and momentum in harmonic oscillators. Similar to the harmonic oscillator, there are also displacement operators which lead to a shift in angular-position or angular-momentum bases. In particular, the momentum-displacement operator  $X(m) = e^{im\hat{\theta}}$  is labeled by an integer  $m \in \mathbb{Z}$ , whereas the phase-displacement operator  $Z(\phi) = e^{i\phi\hat{\ell}}$  is characterized by a continuous angle  $\phi \in [0, 2\pi]$ . The action of these operators on the system's bases is as follows:

$$\begin{aligned} X(m)|\theta\rangle &= e^{im\theta} |\theta\rangle, & X(m)|\ell\rangle &= |\ell + m\rangle \\ Z(\phi)|\theta\rangle &= |\theta - \phi\rangle, & Z(\phi)|\ell\rangle &= e^{i\phi\ell} |\ell\rangle \end{aligned} \quad (2)$$

In this regard,  $X(m)$  and  $Z(\phi)$  have roles similar to Pauli operators and we call them generalized Pauli operators. The commutation relation between these operators, which is very canonical in rotor-based error-correction codes and governs the control of logical operators in this system, is given by the following expression:

$$X(m)Z(\phi) = e^{-im\phi} Z(\phi)X(m) \quad (3)$$

This relation shows that the operators  $X(m)$  and  $Z(\phi)$  commute only when  $m\phi = 0 \pmod{2\pi}$ . Now, we are ready to introduce a toric-rotor code which is typically defined on a two-dimensional square lattice with periodic boundary conditions (i.e., a torus). In this model, each edge of the lattice hosts a quantum rotor instead of a qubit, and the code structure is determined by the stabilizer group, whose generators are the face and vertex

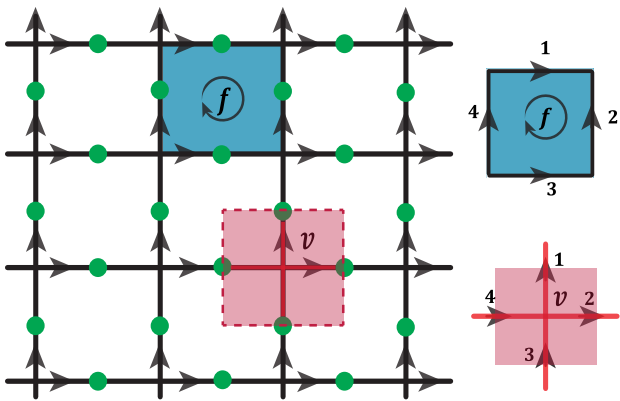


FIG. 1. Two-dimensional square lattice of the toric-rotor code. Quantum rotors (green circles) reside on the edges of the lattice, with a fixed orientation assigned to each edge. A blue square represents a face stabilizer, constructed as the product of the corresponding operators around the face; for example,  $B_f(m) = X_1(m)X_2(-m)X_3(-m)X_4(m)$ . A red square represents a vertex stabilizer, constructed as the product of the corresponding operators on the edges incident to the vertex; for example,  $A_v(\phi) = Z_1(\phi)Z_2(\phi)Z_3(-\phi)Z_4(-\phi)$ .

stabilizers. In order to define stabilizers, we consider an orientation to each edge of the lattice as shown in Fig. 1. Then Face stabilizers are constructed as the product of  $X(m)$  operators around each face of the lattice:

$$B_f(m) = \prod_{e \in \partial f} X_e(m)^{\varepsilon_{e,f}} = e^{im \sum_{e \in \partial f} \varepsilon_{e,f} \hat{\theta}_e} \quad (4)$$

where  $\varepsilon_{e,f} = \pm 1$  specifies the orientation of an edge, such that  $\varepsilon_{e,f}$  is set to +1 (-1) if the orientation of the corresponding edge matches clockwise (anticlockwise) circulation around the associated face; see Fig. 1. Vertex stabilizers are constructed as the product of  $Z(\phi)$  operators incident on each vertex:

$$A_v(\phi) = \prod_{e \in v} Z_e(\phi)^{\varepsilon_{e,v}} = e^{i\phi \sum_{e \in v} \varepsilon_{e,v} \hat{\ell}_e} \quad (5)$$

where  $\varepsilon_{e,v} = \pm 1$  is set to -1 (+1) if the corresponding edge is incoming to (outgoing from) the associated vertex; see Fig. 1. The specific definition of stabilizers according to orientation of the lattice edges ensures that the vertex and face stabilizer operators commute, that is,  $[A_v(\phi), B_f(m)] = 0$ . In particular, it is simple to check that for any arbitrary orientation attached to edges the commutation relation is held. However, in this work, we restrict our attention to the specific orientation shown in Fig. 1.

Due to the torus topology, the subspace of the code includes two logical rotors. In order to characterize logical states of the code, note that the logical subspace consists of all states that are stabilized by every vertex  $A_v(\phi)$  and face stabilizer  $B_f(m)$ , with eigenvalue +1. Starting from the configuration in which all rotors have angular momentum  $\ell = 0$ , one of the logical states can be expressed

in the following unnormalized form:

$$\begin{aligned} |G\rangle &= \prod_f \left( \sum_{n_f \in \mathbb{Z}} B_f(n_f) \right) |\ell = 0\rangle^{\otimes M} \\ &= \prod_f \left( \sum_{n_f \in \mathbb{Z}} e^{in_f \sum_{e \in \partial f} \varepsilon_{e,f} \hat{\theta}_e} \right) |\ell = 0\rangle^{\otimes M} \end{aligned} \quad (6)$$

Here  $M$  refers to number of rotors,  $\prod_f$  refers to a product corresponding to all independent faces of the lattice and  $n_f \in \mathbb{Z}$  is an integer corresponding to each face  $f$ . The above state can also be defined as the limit of a normalized state. As discussed in [44, 46], one can use a standard regularization procedure by applying a Gaussian envelope to the ideal state:

$$|G_{\text{phys}}\rangle = \mathcal{N}_\Delta \prod_f \left( \sum_{n_f \in \mathbb{Z}} e^{-\frac{\Delta}{2} n_f^2} B_f(n_f) \right) |\ell = 0\rangle^{\otimes M}, \quad (7)$$

where  $\Delta > 0$  is the regularization parameter and  $\mathcal{N}_\Delta$  is a normalization constant proportional to a Jacobi theta function. In the limit  $\Delta \rightarrow 0$ , we recover the ideal state given in Eq. (6).

Now let us go back to the ideal state. owing to the topology of the torus, there exist two operators corresponding to non-contractible loops around the torus that commute with all stabilizers but are not members of the stabilizer group i.e., they cannot be generated by any product of stabilizers. As shown in Fig. 2, we denote these non-trivial loop operators by  $T_x(m)$  and  $T_y(m')$ :

$$\begin{aligned} T_x(m) &= \prod_{e \in \mathcal{C}_x} X_e(m) = e^{im \sum_{e \in \mathcal{C}_x} \hat{\theta}_e} \\ T_y(m') &= \prod_{e \in \mathcal{C}_y} X_e(m') = e^{im' \sum_{e \in \mathcal{C}_y} \hat{\theta}_e} \end{aligned} \quad (8)$$

Here,  $\mathcal{C}_x$  and  $\mathcal{C}_y$  denote the non-contractible loops along the horizontal and vertical directions of the torus, respectively, and  $m$  and  $m'$  are integers. Applying these operators to the reference logical state  $|G\rangle$  maps the system to another orthogonal sector within the code space. The other logical states of the toric-rotor code can be generated from them as follows:

$$|\Phi_{m,m'}\rangle = T_1(m) T_2(m') |G\rangle \quad (9)$$

Unlike qubit codes, in which the dimension of subspace code is finite, the number of logical states in this model is countably infinite, reflecting the compact nature of the position variable  $\hat{\theta}$  and the unbounded spectrum of the momentum variable  $\hat{\ell}$ . Each pair  $(m, m')$  specifies a distinct topological sector. Since no local operator can distinguish these states from one another, one should define the dual non-local operators  $W_{\bar{x}}(\phi)$  and  $W_{\bar{y}}(\phi')$  on paths that intersect the non-contractible loops associated with

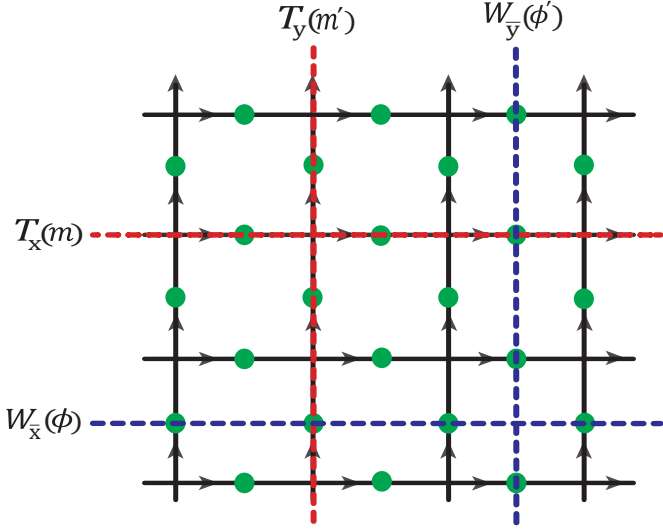


FIG. 2. Non-local operators in the toric-rotor code. The red lines denote the non-contractible loops  $T_x(m)$  and  $T_y(m')$  along the horizontal and vertical lattice directions, formed by products of the corresponding operators. The blue lines denote the operators  $W_{\bar{x}}(\phi)$  and  $W_{\bar{y}}(\phi')$ , defined along horizontal and vertical paths of the dual lattice and intersecting the non-contractible loops.

the  $T$  operators, as shown in Fig. 2, as follows:

$$\begin{aligned} W_{\bar{x}}(\phi) &= \prod_{e \in C_{\bar{x}}} Z_e(\phi) = e^{i\phi \sum_{e \in C_{\bar{x}}} \hat{\ell}_e}, \\ W_{\bar{y}}(\phi') &= \prod_{e \in C_{\bar{y}}} Z_e(\phi') = e^{i\phi' \sum_{e \in C_{\bar{y}}} \hat{\ell}_e} \end{aligned} \quad (10)$$

where  $C_{\bar{x}}$  and  $C_{\bar{y}}$  denote non-contractible loops on the dual lattice, acting only on the edges intersected by the corresponding primal loops. In the basis  $|\Phi_{m,m'}\rangle$ , the  $T$  operators act as shift operators between different topological sectors, whereas the action of the  $W$  operators on this state yields a phase proportional to the corresponding integer label. Their action is given by:

$$\begin{aligned} T_x(k) |\Phi_{m,m'}\rangle &= |\Phi_{m+k,m'}\rangle \\ T_y(k') |\Phi_{m,m'}\rangle &= |\Phi_{m,m'+k'}\rangle \\ W_{\bar{x}}(\varphi) |\Phi_{m,m'}\rangle &= e^{im'\varphi} |\Phi_{m,m'}\rangle \\ W_{\bar{y}}(\varphi') |\Phi_{m,m'}\rangle &= e^{im\varphi'} |\Phi_{m,m'}\rangle \end{aligned} \quad (11)$$

We also note that the code space can be expressed in terms of the basis constructed from the  $W$  operators. Since in the toric-rotor code the Hilbert space has a composite structure, one may employ a continuous phase basis  $(\phi)$  to store information rather than the discrete momentum basis  $(m)$ . By summing over all integers  $m$  and  $m'$  with the fuzzy weights  $e^{im\phi}$  and  $e^{im'\phi'}$ , we obtain a new basis  $|\Psi_{\phi,\phi'}\rangle$ , in which the roles of the  $T$  and  $W$  operators are interchanged. This basis is given by:

$$|\Psi_{\phi,\phi'}\rangle = \sum_m e^{im\phi} T_x(m) \sum_{m'} e^{im'\phi'} T_y(m') |G\rangle \quad (12)$$

In this basis, the  $T$  operators contribute only a phase, whereas the  $W$  operators act as shift operators:

$$\begin{aligned} T_x(k) |\Psi_{\phi,\phi'}\rangle &= e^{-ik\phi} |\Psi_{\phi,\phi'}\rangle \\ T_y(k') |\Psi_{\phi,\phi'}\rangle &= e^{-ik'\phi'} |\Psi_{\phi,\phi'}\rangle \\ W_{\bar{x}}(\varphi) |\Psi_{\phi,\phi'}\rangle &= |\Psi_{\phi,\phi'+\varphi}\rangle \\ W_{\bar{y}}(\varphi') |\Psi_{\phi,\phi'}\rangle &= |\Psi_{\phi+\varphi',\phi'}\rangle \end{aligned} \quad (13)$$

In other words, the above nonlocal operators play the role of logical generalized Pauli gates in the logical subspace. We emphasize that the topological sectors of the logical subspace are protected by topology due to the nonlocal nature of the logical operators, since it is highly unlikely for a local perturbation to generate a nonlocal operator. However, because of the continuity of the phase variable, a nonlocal operator with a very small weight can also act as a logical gate, thereby posing significant challenges for error correction in such codes. In this paper, we consider this problem by using a classical-quantum mapping between the toric-rotor code and the 2D classical  $XY$  model, which provides an important tool for studying correctability in the toric-rotor code.

### III. MAPPING TO CLASSICAL $XY$ MODEL

In order to investigate a quantum-classical correspondence, we introduce a quantum formalism for the partition function of classical  $XY$  model. The Hamiltonian of this model is defined as follows:

$$H = - \sum_{\langle ij \rangle} \cos(\theta_i - \theta_j) \quad (14)$$

Here  $\theta_i$  denotes the spin angle at vertex  $i$ , as shown in Fig. 3, and the Hamiltonian involves a sum over nearest-neighbor pairs on the square lattice with periodic boundary conditions. The partition function of the model is given by

$$\mathcal{Z} = \int_0^{2\pi} \prod_{i=1}^N \frac{d\theta_i}{2\pi} \exp\left(\beta \sum_{\langle ij \rangle} \cos(\theta_i - \theta_j)\right) \quad (15)$$

Here,  $N$  refers to number of spins and  $\beta$  denotes the inverse temperature  $1/T$ , where we set the Boltzmann constant  $k_B$  to 1. We assign an orientation to each edge of the lattice and, for each directed edge  $e$ , define a new variable  $\Theta_e \equiv \theta_i - \theta_j$ , where  $i$  and  $j$  denote the vertices corresponding to the starting and ending points of the edge. We then associate these variables with the edges of the lattice and refer to them as edge variables. Next, we express the partition function in terms of these edge variables instead of the original vertex variables. However, the edge variables  $\Theta_e$  are not independent and must satisfy several geometric constraints. These constraints are incorporated into the partition function through delta-function. The partition function can then be rewritten in terms of these new variables as follows:

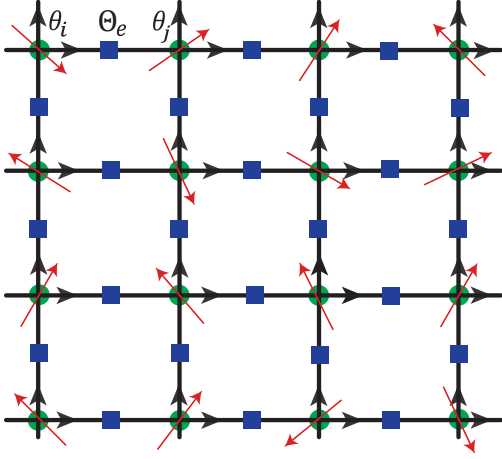


FIG. 3. Square-lattice representation of the two-dimensional XY model. An orientation is assigned to each lattice edge, and the partition function is rewritten by replacing vertex variables  $\theta$  with edge variables  $\Theta_e$ . Each edge variable  $\Theta_e$  (blue squares) is associated with an oriented edge  $e$  connecting vertices  $i$  and  $j$ .

$$\mathcal{Z} = \int_{-\pi}^{\pi} \prod_e^M \frac{d\Theta_e}{2\pi} e^{\beta \sum_e \cos(\Theta_e)} \left[ \prod_f^{N-1} \delta_{2\pi}^f \right] \left[ \delta_{2\pi}^{C_x} \right] \left[ \delta_{2\pi}^{C_y} \right] \quad (16)$$

Where  $\delta_{2\pi}^f = \delta_{2\pi} \left( \sum_{e \in \partial f} \varepsilon_{e,f} \Theta_e \right)$  is a periodic delta function which imposes the constraint that the sum of the edge variables around each face of the lattice (i.e., each closed loop) is equal to  $2\pi n$  with  $n \in \mathbb{Z}$ , see Fig. 4. The factor  $\varepsilon_{e,f} = \pm 1$  specifies the orientation of each edge in the traversal of the loop. Similarly,  $\delta_{2\pi}^{C_x} = \delta_{2\pi} \left( \sum_{e \in C_x} \Theta_e \right)$  and  $\delta_{2\pi}^{C_y} = \delta_{2\pi} \left( \sum_{e \in C_y} \Theta_e \right)$  impose the constraints associated with periodic boundary conditions. These conditions require that the sum of the edge variables along each non-contractible loop of the lattice be an integer multiple of  $2\pi$ . In the next step, we notice that the periodic delta function can be written as a discrete Fourier series,

$$\delta_{2\pi}(x) = \sum_{m \in \mathbb{Z}} \delta(x - 2\pi m) = \frac{1}{2\pi} \sum_{q \in \mathbb{Z}} e^{iqx} \quad (17)$$

Using this representation, the partition function can be written in the form

$$\mathcal{Z} = \int_{-\pi}^{\pi} \prod_{e=1}^M \frac{d\Theta_e}{2\pi} \exp\left(\beta \sum_{e=1}^M \cos(\Theta_e)\right) \mathcal{W}_b \mathcal{W}_l \quad (18)$$

where

$$\mathcal{W}_b = \prod_{f=1}^{N-1} \left( \frac{1}{2\pi} \sum_{n_f \in \mathbb{Z}} e^{in_f \sum_{e \in \partial f} \varepsilon_{e,f} \Theta_e} \right) \quad (19)$$

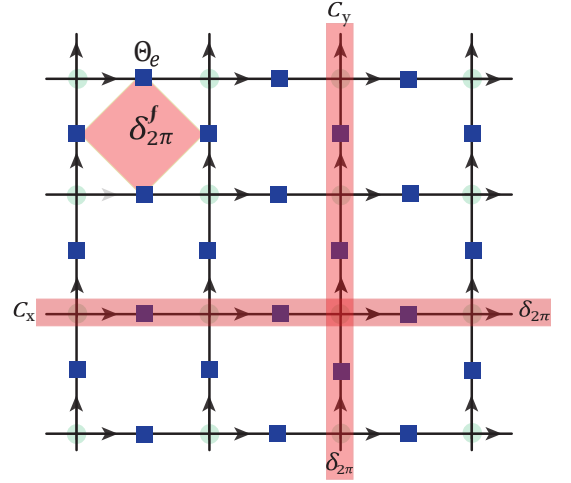


FIG. 4. Geometric representation of the constraints on the edge variables in the rewritten partition function [Eq. (16)].

The symbol  $\delta_{2\pi}^f$  (diamond-shaped region) denotes the local plaquette constraint, enforcing that the oriented sum of edge variables around any closed loop equals an integer multiple of  $2\pi$ . The horizontal and vertical colored bands indicate non-local constraints imposed by periodic boundary conditions.

where we have replaced delta functions corresponding to each face with a Fourier series and  $n_f$  refers to a variable corresponding to a face  $f$  and

$$\mathcal{W}_l = \frac{1}{4\pi^2} \left( \sum_{m \in \mathbb{Z}} e^{im \sum_{e \in C_x} \Theta_e} \right) \left( \sum_{m' \in \mathbb{Z}} e^{im' \sum_{e \in C_y} \Theta_e} \right) \quad (20)$$

has been replaced instead of delta functions corresponding to non-trivial loops.

Now we introduce a quantum formalism for the above relation. To this end, we first use a simple lemma that the integral of an arbitrary function  $f(\Theta)$  can be written in the following form:

$$\langle \ell = 0 | f(\hat{\Theta}) | \ell = 0 \rangle = \int_{-\pi}^{\pi} \frac{d\Theta}{2\pi} f(\Theta) \quad (21)$$

where  $|\ell = 0\rangle = \frac{1}{\sqrt{2\pi}} \int_{-\pi}^{\pi} d\Theta |\Theta\rangle$  denotes the angular-momentum eigenstate with eigenvalue  $\ell = 0$ , and where  $|\Theta\rangle$  are the eigenstates of the angular operator  $\hat{\Theta}$  in the interval  $[-\pi, \pi]$  and satisfy the relation  $\langle \Theta' | \Theta \rangle = \delta(\Theta' - \Theta)$ . This lemma is simply proved by applying the operator  $f(\hat{\Theta})$  to the state  $|\ell = 0\rangle$  and using the fact that  $f(\hat{\Theta}) |\Theta\rangle = f(\Theta) |\Theta\rangle$ . It can also be extended to a function of several variables  $f(\{\Theta_e\})$  in the following form:

$$\int_{-\pi}^{\pi} \prod_{e=1}^M \frac{d\Theta_e}{2\pi} f(\{\Theta_e\}) = {}^M \langle \ell = 0 | f(\{\hat{\Theta}_e\}) | \ell = 0 \rangle^{\otimes M}. \quad (22)$$

We now use the above formalism for the partition function in Eq. (18). In particular, notice that the terms  $\mathcal{W}_b$

and  $\mathcal{W}_l$  are replaced by the following quantum operators:

$$\hat{\mathcal{W}}_b = \prod_{f=1}^{N-1} \left( \frac{1}{2\pi} \sum_{n_f \in \mathbb{Z}} e^{in_f \sum_{e \in \partial f} \varepsilon_{e,f} \hat{\Theta}_e} \right)$$

$$\hat{\mathcal{W}}_l = \frac{1}{4\pi^2} \left( \sum_{m \in \mathbb{Z}} e^{im \sum_{e \in C_x} \hat{\Theta}_e} \right) \left( \sum_{m' \in \mathbb{Z}} e^{im' \sum_{e \in C_y} \hat{\Theta}_e} \right) \quad (23)$$

and accordingly, the partition function is written in the form:

$$\mathcal{Z} = \frac{1}{(2\pi)^{N+1}} M^{\otimes} \langle \ell = 0 | e^{\beta \sum_e \cos \hat{\Theta}_e} \left( \hat{\mathcal{W}}_l \hat{\mathcal{W}}_b \right) | \ell = 0 \rangle^{\otimes M} \quad (24)$$

Then we notice that  $\hat{\mathcal{W}}_b | \ell = 0 \rangle^{\otimes M}$  is the same as the toric-rotor code state  $|G\rangle$  in Eq. (6). On the other hand,  $\hat{\mathcal{W}}_l$  can also be written in terms of logical operators  $T_x(m)$  and  $T_y(m')$  in the toric-rotor code in the form of  $\hat{\mathcal{W}}_l = \sum_{m,m'} T_x(m) T_y(m')$ . In this regard, by comparing with Eq. (12), it is simply concluded that  $\hat{\mathcal{W}}_l |G\rangle$  is equal to the logical state  $|\Psi_{0,0}\rangle$  in the toric-rotor code. Finally, the partition function of the XY model is related to the toric-rotor code state as follows

$$\mathcal{Z} = \frac{1}{(2\pi)^{N+1}} \langle \alpha | \Psi_{0,0} \rangle \quad (25)$$

where  $|\alpha\rangle = \prod_e e^{\beta \cos \hat{\Theta}_e} | \ell = 0 \rangle$  is a product state. In this formulation, the partition function of classical XY model is expressed as the inner product of a product state and a logical state of the toric-rotor code. We note that the classical XY model has been extensively investigated in the context of topological order in classical systems, where it exhibits a KT phase transition at a critical temperature. The main question, then, is how to interpret the right-hand side of Eq. (25) when a logical state of the toric-rotor code appears. To this end, we write  $|\alpha\rangle$  as

$$|\alpha\rangle = \frac{1}{\sqrt{2\pi}} \int_{-\pi}^{\pi} d\Theta e^{\beta \cos \Theta} |\Theta\rangle \quad (26)$$

If we express  $|\Theta\rangle$  as  $|\Theta\rangle = e^{i\Theta \hat{\ell}} |\Theta = 0\rangle$ , then the state  $|\alpha\rangle$  becomes

$$|\alpha\rangle = \frac{1}{\sqrt{2\pi}} \left[ \int_0^{2\pi} d\Theta e^{\beta \cos \Theta} e^{i\Theta \hat{\ell}} \right] |\Theta = 0\rangle \quad (27)$$

According to this representation, the effect of state  $|\alpha\rangle$  to the logical ground state  $|\Psi_{0,0}\rangle$  can be interpreted as applying noise  $e^{i\Theta \hat{\ell}}$ , characterized by a specific probability distribution proportional to  $e^{\beta \cos \Theta}$ . We investigate this interpretation in the next section by considering the toric-rotor code in the presence of noise.

#### IV. PHASE TRANSITION IN NOISY TORIC-ROTOR CODE

In this section, we consider toric-rotor code in presence of a particular noise. We consider phase-shift noise which is described by applying generalized pauli operator  $Z$  which shifts the phase of a quantum state  $|\phi\rangle$  by an angle  $\Theta$ :

$$Z(\Theta) = e^{i\Theta \hat{\ell}} \quad (28)$$

Unlike qubit systems, where errors are typically discrete, the phase variable  $\Theta$  in rotor systems is continuous, so that any nonzero value of  $\Theta$  constitutes an error. However, different phase shifts do not occur with equal probability. We assume that each rotor independently experiences a  $Z$ -type error distributed according to a probability density  $P(\Theta)$ . Since small phase errors are much more likely than large phase errors (i.e., those close to  $\pi$ ), the von Mises probability distribution [43] provides a physically appropriate model for continuous phase noise and takes the form:

$$P(\Theta) = \frac{e^{\frac{\cos \Theta}{\sigma}}}{2\pi I_0(\sigma)} \quad (29)$$

where  $I_0(\sigma)$  is the normalization factor and denotes the modified Bessel function of the first kind of order zero. This distribution is well suited for modeling phase errors in rotor-based codes because it respects the periodicity of the phase variable  $\Theta$  and reduces to a Gaussian distribution in the limit of small  $\Theta$ .

We now assume that the initial state of the system is  $\rho_0 = |\Psi_{0,0}\rangle \langle \Psi_{0,0}|$ . Applying noise to the system is described by a quantum channel in the following Kraus representation:

$$\mathcal{E}(\rho_0) = \int \prod_e d\Theta_e P_e(\Theta_e) \prod_e Z_e(\Theta_e) \rho_0 \prod_e Z_e^\dagger(\Theta_e) \quad (30)$$

An important quantity is the probability that the system remains in the state  $|\Psi_{0,0}\rangle$  after applying the noise. This probability can be obtained by computing the fidelity between the noisy state and the original state  $|\Psi_{0,0}\rangle$ , which is defined as

$$\mathcal{F} = \langle \Psi_{0,0} | \mathcal{E}(\rho_0) | \Psi_{0,0} \rangle \quad (31)$$

This expression is nonzero only when the phase variables  $\{\Theta_e\}$  satisfy specific constraints such that the operator  $\prod_e Z_e(\Theta_e)$  belongs to the stabilizer group of the state  $|\Psi_{0,0}\rangle$ . To this end,  $\prod_e Z_e(\Theta_e)$  must commute with the stabilizer operators  $B_f(m)$  as well as the logical operators  $T_x(m)$  and  $T_y(m')$ . The requirement that  $\prod_e Z_e(\Theta_e)$  commutes with each of these operators imposes corresponding constraints, which are enforced through periodic delta functions. As a result, the fidelity can be writ-

ten as

$$\mathcal{F} = \frac{1}{(2\pi I_0(\sigma))^M} \int \prod_e d\Theta_e e^{\frac{\sum_e \cos \Theta_e}{\sigma}} \left[ \prod_f^{N-1} \delta_{2\pi} \right] \left[ \delta_{2\pi}^{C_x} \right] \left[ \delta_{2\pi}^{C_y} \right] \quad (32)$$

By comparing with Eq. (16) and substituting  $1/\sigma = \beta$ , this expression is proportional to the partition function of the two-dimensional  $XY$  model. Therefore, we have:

$$\mathcal{F} = \frac{1}{[I_0(\sigma)]^M} \mathcal{Z} \quad (33)$$

Because the partition function of the two-dimensional  $XY$  model, and hence its free energy, exhibits an essential singularity at the KT transition temperature  $T_c \approx 0.89$  [47, 48], the corresponding quantum state fidelity is expected to display analogous non-analytic behavior at a critical width  $\sigma_c$ . The quantum model therefore undergoes a KT-type phase transition and we should identify a physical quantity that characterizes this transition. Guided by the established mapping, we consider the order parameter of the classical  $XY$  model and then look for its quantum analogue. First, we notice that by the Mermin-Wagner theorem [49], systems with continuous symmetry and short-range interactions in  $d \leq 2$  lack long-range order at any finite temperature, implying vanishing magnetization for all  $T > 0$ . As a result, magnetization cannot distinguish the low-temperature phase with quasi-long-range order from the high-temperature disordered phase in the  $XY$  model. The KT transition is instead characterized by the spin stiffness (helicity modulus), which quantifies the system's response to a twist in the boundary conditions [50]. To define the spin stiffness, one considers a Hamiltonian similar to Eq. (14) with a twist introduced by modifying the boundary couplings to  $-J \cos(\theta_i - \theta_j - \phi)$ , as shown in Fig. 5. Here,  $\phi$  is the twist angle, and the original model is recovered for  $\phi = 0$ . The twisted Hamiltonian can be written as:

$$H_\phi = -J \sum_e \cos(\Theta_e - \delta_e \phi), \quad (34)$$

where  $\Theta_e = \theta_i - \theta_j$ ,  $\delta_e = 1$  for edges  $e$  corresponding to the twisted boundary and  $\delta_e = 0$  otherwise. The partition function and free energy of the twisted model are functions of  $\phi$ , where  $\mathcal{A}_\phi = -T \ln \mathcal{Z}_\phi$ . In a macroscopic phase with quasi-long-range order, imposing a twist in the boundary conditions leads to an increase in the free energy of the system  $\Delta \mathcal{A} = \mathcal{A}_\phi - \mathcal{A}_0$ . For a given angle  $\phi$ , spin stiffness is defined in terms of this increase as follows:

$$\rho_s(\phi) = \frac{2 \Delta \mathcal{A}}{\phi^2} L^{2-d}. \quad (35)$$

where  $d$  is the spatial dimension of the system,  $L$  is the linear system size and  $\rho_s$  denotes the spin stiffness [51]. In the limit  $\phi \rightarrow 0$ , this quantity can be expressed as

$$\rho_s = \left( \frac{\partial^2 \mathcal{A}}{\partial \phi^2} \right)_{\phi=0} L^{2-d} \quad (36)$$

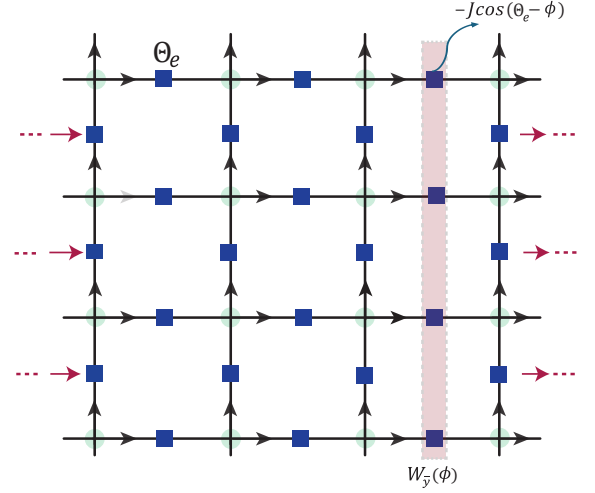


FIG. 5. Schematic illustration of twisted periodic boundary conditions for the  $XY$  model and its interpretation in the toric-rotor code. The twist is introduced by imposing a phase shift  $\phi$  on the edges crossing a specified boundary (indicated by the red shaded bar corresponding to a non-contractible loop  $C_{\bar{y}}$ ). For these edges, which  $\delta_e = 1$ , the interaction term in the Hamiltonian changes to  $-J \cos(\Theta_e - \phi)$  where  $\Theta_e = \theta_i - \theta_j$ . Using the quantum formalism, the twist corresponds to applying  $W_{\bar{y}}(\phi)$  to the initial state  $|\Psi_{0,0}\rangle$  in the presence of noise.

In the disordered phase, the system does not resist boundary twists and the spin stiffness vanishes,  $\rho_s = 0$ , whereas in the ordered phase elastic spin correlations lead to a finite stiffness,  $\rho_s \neq 0$ . In two dimensions, it has been shown [52] that  $\rho_s$  exhibits a discontinuous jump from a finite value to zero at the transition temperature  $T_c$  (Fig. 6).

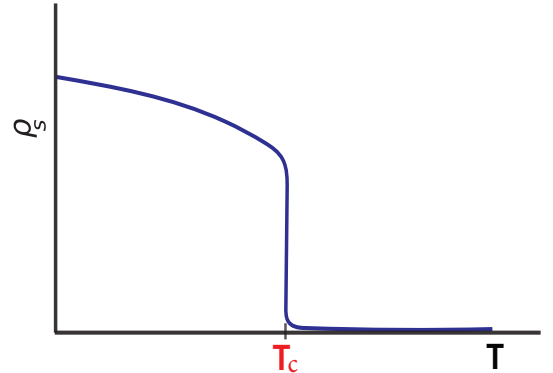


FIG. 6. Spin stiffness  $\rho_s$  as a function of temperature  $T$  for the two-dimensional  $XY$  model [53]. At low temperatures ( $T < T_c$ ),  $\rho_s$  remains finite, reflecting the system's elastic response to a boundary twist. In the thermodynamic limit,  $\rho_s$  exhibits a universal discontinuous jump from a finite value to zero at the critical temperature  $T_c \approx 0.89$ , signaling the transition from the quasi-long-range ordered phase to the disordered phase.

## V. SPIN STIFFNESS AND A RESILIENCE ORDER PARAMETER:

Since spin stiffness is a suitable order parameter for  $XY$  model, in this section we look for its quantum analogue by using the classical-to-quantum mapping. To this end, we focus on partition function of the twisted model Eq. (34) and find a quantum formalism. We write the partition function in the presence of a twist analogously to that of the untwisted case:

$$\mathcal{Z}_\phi = \int_{-\pi}^{\pi} \prod_e^M \frac{d\Theta_e}{2\pi} e^{\beta \sum_e \cos(\Theta_e - \delta_e \phi)} \left[ \prod_f^{N-1} \delta_{2\pi} \right] \left[ \delta_{2\pi}^{C_x} \right] \left[ \delta_{2\pi}^{C_y} \right] \quad (37)$$

Then, similar to Eq. (24) for the untwisted model, the partition function of the twisted model can be written in quantum formalism as follows:

$$\mathcal{Z}_\phi = M^\otimes \langle \ell = 0 | \prod_e e^{\beta \cos(\hat{\Theta}_e - \delta_e \phi)} | \Psi_{0,0} \rangle \quad (38)$$

Next, using the fact that

$$e^{\beta \cos(\hat{\Theta}_e - \delta_e \phi)} | \ell = 0 \rangle = \frac{1}{\sqrt{2\pi}} \int_{-\pi}^{\pi} e^{\beta \cos(\Theta_e - \delta_e \phi)} d\Theta_e | \Theta_e \rangle \quad (39)$$

and the change of variables  $\Theta'_e = \Theta_e - \delta_e$ , one finds that

$$\mathcal{Z}_\phi = \frac{1}{(2\pi)^{N+1}} \langle \alpha | \prod_e Z_e(\delta_e \phi) | \Psi_{0,0} \rangle \quad (40)$$

According to this equation, the twist angle added in the Hamiltonian of the  $XY$  model leads to an operator  $\prod_e Z_e(\delta_e \phi)$  in the quantum formalism. As shown in Fig. 5, the twisted boundary is crossed by a non-contractible loop  $C_{\bar{y}}$ . Therefore,  $\prod_e Z_e(\delta_e \phi)$  is the same as non-contractible operator  $W_{\bar{y}}(\phi)$  defined in Eq. (10) as a logical operator of toric-rotor code. In particular, according to the definition of the logical states in Eq. (13) we have  $\prod_e Z_e(\delta_e \phi) | \Psi_{0,0} \rangle = | \Psi_{\phi,0} \rangle$ . In this regard, we conclude that the partition function of the  $XY$  model in the presence of a twist can be expressed as follows:

$$\mathcal{Z}_\phi = \frac{1}{(2\pi)^{N+1}} \langle \alpha | \Psi_{\phi,0} \rangle \quad (41)$$

This relationship implies that by applying a twist to the  $XY$  model, the system is mapped onto another logical state of the toric-rotor code. We again consider the effect of noise on the state  $| \Psi_{0,0} \rangle$  and calculate its fidelity with respect to state  $| \Psi_{\phi,0} \rangle$ , as follows:

$$\mathcal{F}_\phi = \langle \Psi_{\phi,0} | \mathcal{E}(\rho_0) | \Psi_{\phi,0} \rangle \quad (42)$$

This fidelity is equal to a probability that the initial logical state is transformed to another logical state in effect of the noise. By replacing  $| \Psi_{\phi,0} \rangle$  from Eq. (13), the fidelity  $\mathcal{F}_\phi$  can be written as

$$\mathcal{F}_\phi = \langle \Psi_{0,0} | \mathcal{E}_\phi(\rho_0) | \Psi_{0,0} \rangle \quad (43)$$

where  $\mathcal{E}_\phi(\rho_0)$  is defined analogously to  $\mathcal{E}(\rho_0)$  in Eq. (30), except that the operator  $\prod_e Z_e(\Theta_e)$  is replaced by  $\prod_e Z_e(\Theta_e + \delta_e \phi)$ . By performing the change of variables  $\Theta'_e = \Theta_e + \delta_e \phi$ , the following expression for  $\mathcal{E}_\phi(\rho_0)$  is obtained:

$$\mathcal{E}_\phi(\rho_0) = \int \prod_e d\Theta'_e P_e(\Theta'_e - \delta_e \phi) \prod_e Z_e(\Theta'_e) \rho_0 \prod_e Z_e^\dagger(\Theta'_e) \quad (44)$$

Substituting this expression into Eq. (43) and using the same argument as before, we find that  $\mathcal{F}_\phi$  is proportional to the partition function of the  $XY$  model in the presence of a twist (see Eq. (37)). Consequently, one obtains

$$\mathcal{F}_\phi = \frac{1}{[I_0(\sigma)]^M} \mathcal{Z}_\phi \quad (45)$$

Now, let us provide a physical interpretation of the results derived from the quantum formalism. In particular, notice that we have a toric-rotor code initialized in the logical state  $| \Psi_{0,0} \rangle$ . Then, under the effect of phase-shift noise applied to the rotors, the initial state is converted into a mixture of different logical states and excited states of the code. In this regard, our results show that probability of each one of logical states  $| \Psi_{\phi,0} \rangle$  in the final mixture is proportional to partition function of the  $XY$  model with twist angle  $\phi$ . In this regard, we may interpret the above fidelity as a gate fidelity, in the sense that it quantifies fidelity between noise-induced operator and the logical gate  $W_{\bar{y}}$ .

In the next step, we connect the above fidelity relation to spin stiffness in the  $XY$  model. To this end, we take the logarithm of both sides and multiply by the thermal factor  $T$ ; neglecting the constant term then yields the following relationship between the logarithm of the fidelity and the free energy ( $\mathcal{A}_\phi$ ) [54]:

$$-T \ln \mathcal{F}_\phi = \mathcal{A}_\phi. \quad (46)$$

Next, we take the second derivative of this equation with respect to the phase parameter  $\phi$ :

$$-\left( \frac{\partial^2 \ln \mathcal{F}_\phi}{\partial \phi^2} \right)_{\phi=0} = \frac{1}{T} \left( \frac{\partial^2 \mathcal{A}_\phi}{\partial \phi^2} \right)_{\phi=0} \quad (47)$$

According to Eq. (36), the right-hand side of the above equation is the same as the spin stiffness ( $\rho_s$ ) in the  $XY$  model while the left-hand side corresponds to the *fidelity susceptibility*, denoted by  $\chi_F$  [55]. Consequently, the relationship between the fidelity susceptibility and the spin stiffness is given by:

$$\chi_F = \frac{L^{d-2}}{T} \rho_s \quad (48)$$

In two dimensions ( $d = 2$ ),  $\chi_F$  is proportional to  $\rho_s$  and is independent of the system size.

It seems that just as  $\rho_s$  measures the stiffness of the classical system with respect to an applied twist,  $\chi_F$  indicates the sensitivity of the logical state in the quantum code to a noise-induced logical gate. In order to

clarify this point, let us return to the relation between fidelity and free energy in Eq. (46). We rewrite this equation as  $\mathcal{F}_\phi = \exp\left(-\frac{\mathcal{A}_\phi}{T}\right)$ . Then, it follows that  $\frac{\mathcal{F}_\phi}{\mathcal{F}} = \exp\left(-\frac{\mathcal{A}_\phi - \mathcal{A}_0}{T}\right)$ . On the other hand, with regard to the relation between free energy and spin stiffness in Eq. (35), we conclude that:

$$\mathcal{F}_\phi = \mathcal{F} \exp\left(-\frac{\rho_s}{2T} \phi^2 L^{d-2}\right). \quad (49)$$

Using the above relation, we can determine the different phases of the noisy toric-rotor code model. First, we consider the high-noise regime when the noise width is greater than  $\sigma_c \approx 0.89$  or the temperature is greater than  $T_c$ . In this phase,  $\rho_s = 0$ , and therefore the fidelity  $\mathcal{F}_\phi$  is equal to  $\mathcal{F}$  for all values of  $\phi$ . On the other hand, we recall that the fidelity  $\mathcal{F}_\phi$  represents the probability that the effect of noise leads to a logical gate  $W_{\bar{y}}(\phi)$ . Therefore, it can be concluded that in the high-noise phase, the toric-rotor mixed state occupies different logical states  $|\Psi_{\phi,0}\rangle$  with equal probabilities. This implies that complete decoherence occurs within the logical subspace when the noise width is greater than  $\sigma_c$ . Conversely, in the low-noise phase, where  $\sigma < \sigma_c$ , since  $\rho_s \neq 0$ ,  $\mathcal{F}_\phi$  is a Gaussian function of  $\phi$  that peaks at  $\phi = 0$  and decays as  $\phi$  increases. This implies that in the low-noise phase, the probability of different logical states is different and the system retains a finite degree of coherence. In other words, the KT phase in the XY model corresponds to a coherent phase for the logical subspace of the toric-rotor code while the disordered phase corresponds to a decoherent phase.

It is also important to characterize this phase using a suitable order parameter. To this end, we define the expectation value  $\langle \cos \phi \rangle$ , which is evaluated with respect to the probability distribution function  $\mathcal{F}_\phi / \int \mathcal{F}_\phi d\phi$ :

$$\lambda = \frac{\int_{-\pi}^{\pi} \cos(\phi) e^{-\frac{\rho_s}{2T} \phi^2} d\phi}{\int_{-\pi}^{\pi} e^{-\frac{\rho_s}{2T} \phi^2} d\phi} \quad (50)$$

According to our argument about behavior of the probability function in different phases, it is expected that  $\lambda$  equals zero in the decoherent phase, while it takes a nonzero value in the coherent phase; therefore, it serves as a suitable order parameter. As shown in Fig. 7, we plot this order parameter by substituting different values of  $\rho_s$  into the probability function, with reference to Fig. 6. It shows that coherence in the logical subspace is close to 1 in the coherent phase and then drops to zero at the critical point of  $\sigma_c$ . In other words, in the coherent phase, the topological sectors show resilience to noise, while in the decoherent phase, they become completely mixed. Accordingly, we may refer to the above phase transition as a resilience phase transition, and we call  $\lambda$  a resilience order parameter. On the other hand, we also recall Eq. (13) where  $e^{-i\phi}$  is the eigenvalue of logical operator  $T_x$  corresponding to  $|\Psi_{\phi,0}\rangle$ . In this regard, we interpret  $\lambda$  as the

expectation value of the logical operator  $\frac{T_x + T_x^\dagger}{2}$ , evaluated in the logical subspace. In particular, non-locality of the above operator implies that nature of the phase transition is topological. In other words, we have found a correspondence between classical and quantum topological orders where we map a classical topological order parameter (spin stiffness) to a quantum topological order parameter.

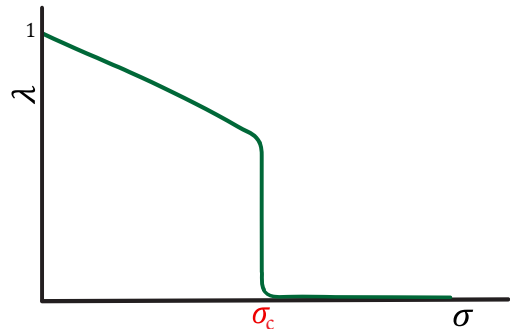


FIG. 7. Resilience order parameter  $\lambda$  as a function of the noise width  $\sigma$ . In the coherent phase, coherence within the logical subspace remains close to unity, indicating the resilience of the topological sectors against noise. At the critical point  $\sigma_c \approx 0.89$ , the system undergoes a resilience phase transition, where  $\lambda$  drops sharply to zero, signaling the onset of the decoherent phase in which the topological sectors become completely mixed.

We then notice that the value of coherence in the resilient phase is not equal to 1. This implies that even in the coherent phase, there is a slight mixing between different topological sectors. This implies that the toric-rotor code is not correctable in the presence of phase-shift noise, because even a very small value of the noise width leads to a logical error that cannot be detected or corrected. In other words, the 2D toric-rotor code does not satisfy the necessary condition for correctability. However, we emphasize that for the toric-rotor code in higher dimensions, correctability remains possible. In particular, as can be seen in Eq. (49), there is a term proportional to  $L^{d-2}$  in the exponential. Accordingly, for  $d > 2$ , as the system size  $L$  goes to  $\infty$ ,  $\mathcal{F}_\phi$  approaches zero for any finite value of  $\phi$ , whereas it is nonzero only for  $\phi = 0$ . This implies that throughout the coherent phase, the resilience order parameter is equal to 1 and therefore satisfies the necessary condition for correctability. In this regard, the critical width  $\sigma_c$  for higher-dimensional toric-rotor codes can be regarded as a threshold, which we call the passive threshold. We should emphasize that this passive threshold is different from the conventional threshold for active error correction. In other words, even when the effect of noise generates only local excitations in the initial topological sector, it is necessary to detect and correct local excitations. However, the error-correction process can also lead to a logical error. Therefore, there is an active threshold in the sense that below it the quan-

tum code is correctable. Notably, the active threshold is generally lower than the passive threshold. As discussed in [43], it is expected that calculation of the active threshold maps to a disordered version of  $XY$  model.

Finally, we note that, as discussed in the definition of the normalized logical state in Eq. (7), the focus of our study was on the limit  $\Delta \rightarrow 0$ . In this regard, it is also interesting to consider the effect of the regularization parameter on correctability. In particular, according to [44], it is expected that situation would be worse in the regularized case. Consequently, for  $d = 2$ , we anticipate that there is no correctable phase, similar to the case  $\Delta \rightarrow 0$ . However, for higher dimensions, where there is a correctable phase for  $\Delta \rightarrow 0$ , we expect that an increment of the regularization parameter leads to a reduction in the value of the passive threshold  $\sigma_c$ .

## VI. CONCLUSION

While quantum formalisms for the partition functions of classical spin models have been extensively studied over the past decades, classical models with continuous variables have received less attention. Here, we introduced a quantum formalism for the partition function of the classical  $XY$  model and showed that it leads to new insights into the toric-rotor code in the presence of phase-shift noise. In particular, we characterized a mixed-state phase transition in the logical subspace of the toric-rotor

code. We showed that this phase transition occurs as the width of the noise increases, in the sense that the noise width plays a role analogous to temperature in the  $XY$  model. We further demonstrated that the spin stiffness of the  $XY$  model is related to the resilience of the toric-rotor code to noise. Using well-known properties of the spin stiffness, we identified a resilience order parameter for characterizing the phase transition in the noisy toric-rotor code. Although our calculations are directly related to the two-dimensional toric-rotor code, our results suggest enhanced resilience to noise for the toric-rotor code in higher dimensions. In particular, the value of the noise width at the transition point can be regarded as a passive threshold below which high-dimensional toric-rotor codes satisfy the necessary condition for correctability. In this regard, the approach introduced in this paper can shed new light on correctability in continuous-variable quantum codes.

Finally, we would like to emphasize that our results establish a mapping between classical and quantum versions of topological phase transitions. This can lead to an interesting cross-fertilization between classical and quantum topological order in the sense that our knowledge of topological order in one case leads to new insights into the other.

## ACKNOWLEDGMENT

We would like to thank Mohammad Nobakht for valuable discussions during several meetings that we had on this work.

- 
- [1] P. W. Shor, Scheme for reducing decoherence in quantum computer memory, *Phys. Rev. A* **52**, R2493 (1995).
- [2] A. M. Steane, Error Correcting Codes in Quantum Theory, *Phys. Rev. Lett.* **77**, 793 (1996).
- [3] D. Gottesman, Stabilizer codes and quantum error correction (1997), arXiv:quant-ph/9705052.
- [4] A. Y. Kitaev, Fault-tolerant quantum computation by anyons, *Annals of Physics* **303**, 2 (2003), arXiv:quant-ph/9707021.
- [5] X. Chen, Z.-C. Gu, and X.-G. Wen, Local unitary transformation, long-range quantum entanglement, wave function renormalization, and topological order, *Phys. Rev. B* **82**, 155138 (2010), arXiv:1004.3835 [cond-mat].
- [6] X.-G. Wen, Zoo of quantum-topological phases of matter, *Rev. Mod. Phys.* **89**, 041004 (2017), arXiv:1610.03911 [cond-mat].
- [7] M. H. Zarei, Robustness of topological quantum codes: Ising perturbation, *Phys. Rev. A* **91**, 022319 (2015).
- [8] C. Nayak, S. H. Simon, A. Stern, M. Freedman, and S. Das Sarma, Non-Abelian anyons and topological quantum computation, *Rev. Mod. Phys.* **80**, 1083 (2008).
- [9] B. M. Terhal, Quantum Error Correction for Quantum Memories, *Rev. Mod. Phys.* **87**, 307 (2015), arXiv:1302.3428 [quant-ph].
- [10] A. G. Fowler, M. Mariantoni, J. M. Martinis, and A. N. Cleland, Surface codes: Towards practical large-scale quantum computation, *Phys. Rev. A* **86**, 032324 (2012), arXiv:1208.0928 [quant-ph].
- [11] A. Jamadagni, H. Weimer, and A. Bhattacharyya, Robustness of Topological Order in the Toric Code with Open Boundaries, *Phys. Rev. B* **98**, 235147 (2018), arXiv:1804.09718 [cond-mat].
- [12] G. Zhu, T. Jochym-O'Connor, and A. Dua, Topological Order, Quantum Codes and Quantum Computation on Fractal Geometries, *PRX Quantum* **3**, 030338 (2022), arXiv:2108.00018 [quant-ph].
- [13] L. A. Oliveira and W. Chen, Robustness of topological order against disorder, *Phys. Rev. B* **109**, 094202 (2024).
- [14] I. Cong, N. Maskara, M. C. Tran, H. Pichler, G. Semeghini, S. F. Yelin, S. Choi, and M. D. Lukin, Enhancing Detection of Topological Order by Local Error Correction, *Nat Commun* **15**, 1527 (2024), arXiv:2209.12428 [quant-ph].
- [15] E. Dennis, A. Kitaev, A. Landahl, and J. Preskill, Topological quantum memory, *Journal of Mathematical Physics* **43**, 4452 (2002), arXiv:quant-ph/0110143.
- [16] C. Wang, J. Harrington, and J. Preskill, Confinement-Higgs transition in a disordered gauge theory and the accuracy threshold for quantum memory, *Annals of Physics* **303**, 31 (2003), arXiv:quant-ph/0207088.
- [17] D. Vodola, M. Rispler, S. Kim, and M. Müller, Fundamental thresholds of realistic quantum error correc-

- tion circuits from classical spin models, *Quantum* **6**, 618 (2022), arXiv:2104.04847 [quant-ph].
- [18] Y. Zhao and D. E. Liu, Extracting error thresholds through the framework of approximate quantum error correction condition, *Phys. Rev. Research* **6**, 043258 (2024).
- [19] S. Sang, Y. Zou, and T. H. Hsieh, Mixed-State Quantum Phases: Renormalization and Quantum Error Correction, *Phys. Rev. X* **14**, 031044 (2024).
- [20] Z. Wang, Z. Wu, and Z. Wang, Intrinsic Mixed-State Topological Order, *PRX Quantum* **6**, 010314 (2025).
- [21] R. Sohal and A. Prem, Noisy Approach to Intrinsically Mixed-State Topological Order, *PRX Quantum* **6**, 010313 (2025).
- [22] R. Fan, Y. Bao, E. Altman, and A. Vishwanath, Diagnostics of mixed-state topological order and breakdown of quantum memory, *PRX Quantum* **5**, 020343 (2024), arXiv:2301.05689 [quant-ph].
- [23] Z. Li and R. S. K. Mong, Replica topological order in quantum mixed states and quantum error correction, *Phys. Rev. B* **111**, 125106 (2025).
- [24] S. Lee and E.-G. Moon, Mixed-state topological order under coherent noise, *PRX Quantum* **6**, 030355 (2025).
- [25] A. Lyons, Understanding Stabilizer Codes Under Local Decoherence Through a General Statistical Mechanics Mapping (2024), arXiv:2403.03955 [quant-ph].
- [26] R. Niwa and J. Y. Lee, Coherent information for CSS codes under decoherence, *Phys. Rev. A* **111**, 032402 (2025), arXiv:2407.02564 [quant-ph].
- [27] Y.-H. Chen and T. Grover, Separability transitions in topological states induced by local decoherence, *Phys. Rev. Lett.* **132**, 170602 (2024), arXiv:2309.11879 [quant-ph].
- [28] J. Y. Lee, Exact Calculations of Coherent Information for Toric Codes under Decoherence: Identifying the Fundamental Error Threshold, *Phys. Rev. Lett.* **134**, 250601 (2025), arXiv:2402.16937 [cond-mat].
- [29] Y. Li and M. P. A. Fisher, Statistical mechanics of quantum error correcting codes, *Phys. Rev. B* **103**, 104306 (2021).
- [30] C. T. Chubb and S. T. Flammia, Statistical mechanical models for quantum codes with correlated noise, *Ann. Inst. Henri Poincaré Comb. Phys. Interact.* **8**, 269 (2021), arXiv:1809.10704 [quant-ph].
- [31] H. Bombin, R. S. Andrist, M. Ohzeki, H. G. Katzgraber, and M. A. Martin-Delgado, Strong Resilience of Topological Codes to Depolarization, *Phys. Rev. X* **2**, 021004 (2012), arXiv:1202.1852 [quant-ph].
- [32] M. V. Den Nest, W. Dür, and H. J. Briegel, Classical spin models and the quantum-stabilizer formalism, *Phys. Rev. Lett.* **98**, 117207 (2007).
- [33] M. H. Zarei and A. Montakhab, Dual correspondence between classical spin models and quantum CSS states, *Phys. Rev. A* **98**, 012337 (2018), arXiv:1710.01902 [quant-ph].
- [34] M. V. den Nest, W. Dür, and H. J. Briegel, Completeness of the classical 2D Ising model and universal quantum computation, *Phys. Rev. Lett.* **100**, 110501 (2008), arXiv:0708.2275 [quant-ph].
- [35] S. Bravyi and R. Raussendorf, On measurement-based quantum computation with the toric code states, *Phys. Rev. A* **76**, 022304 (2007), arXiv:quant-ph/0610162.
- [36] M. H. Zarei and A. Montakhab, Classical criticality establishes quantum topological order, *Phys. Rev. B* **101**, 205118 (2020).
- [37] M. H. Zarei and A. Montakhab, Phase transition in a noisy Kitaev toric code model, *Phys. Rev. A* **99**, 052312 (2019).
- [38] M. H. Zarei and A. Ramezanpour, Noisy Toric code and random bond Ising model: The error threshold in a dual picture, *Phys. Rev. A* **100**, 062313 (2019), arXiv:1911.10494 [quant-ph].
- [39] M. H. Devoret and R. J. Schoelkopf, Superconducting Circuits for Quantum Information: An Outlook, *Science* **339**, 1169 (2013).
- [40] A. L. Grimsmo, J. Combes, and B. Q. Baragiola, Quantum computing with rotation-symmetric bosonic codes, *Phys. Rev. X* **10**, 011058 (2020), arXiv:1901.08071 [quant-ph].
- [41] D. Gottesman, A. Kitaev, and J. Preskill, Encoding a qubit in an oscillator, *Phys. Rev. A* **64**, 012310 (2001).
- [42] V. V. Albert, S. Pascazio, and M. H. Devoret, General phase spaces: From discrete variables to rotor and continuum limits, *J. Phys. A: Math. Theor.* **50**, 504002 (2017), arXiv:1709.04460 [quant-ph].
- [43] C. Vuillot, A. Ciani, and B. M. Terhal, Homological Quantum Rotor Codes: Logical Qubits from Torsion, *Commun. Math. Phys.* **405**, 53 (2024).
- [44] Y. Xu, Y. Wang, and V. V. Albert, Clifford operations and homological codes for rotors and oscillators, *Phys. Rev. A* **110**, 022402 (2024), arXiv:2311.07679 [quant-ph].
- [45] J. M. Martinis, Course 13 Superconducting qubits and the physics of Josephson junctions, in *Les Houches*, Vol. 79 (Elsevier, 2004) pp. 487–520.
- [46] B. Royer, S. Singh, and S. M. Girvin, Stabilization of Finite-Energy Gottesman-Kitaev-Preskill States, *Phys. Rev. Lett.* **125**, 260509 (2020), arXiv:2009.07941 [quant-ph].
- [47] J. M. Kosterlitz and D. J. Thouless, Ordering, metastability and phase transitions in two-dimensional systems, *J. Phys. C: Solid State Phys.* **6**, 1181 (1973).
- [48] R. Gupta and C. F. Baillie, Critical behavior of the two-dimensional XY model, *Phys. Rev. B* **45**, 2883 (1992).
- [49] N. D. Mermin and H. Wagner, Absence of Ferromagnetism or Antiferromagnetism in One- or Two-Dimensional Isotropic Heisenberg Models, *Phys. Rev. Lett.* **17**, 1133 (1966).
- [50] Y.-D. Hsieh, Y.-J. Kao, and A. W. Sandvik, Finite-size scaling method for the Berezinskii-Kosterlitz-Thouless transition, *J. Stat. Mech.* **2013**, P09001 (2013), arXiv:1302.2900 [cond-mat].
- [51] G. Khairnar and T. Vojta, Helicity modulus and chiral symmetry breaking for boundary conditions with finite twist, *Phys. Rev. E* **111**, 024114 (2025), arXiv:2312.04468 [cond-mat].
- [52] P. Minnhagen and B. J. Kim, Direct Evidence of the Discontinuous Character of the Kosterlitz-Thouless Jump, *Phys. Rev. B* **67**, 172509 (2003), arXiv:cond-mat/0304226.
- [53] U. Gerber, W. Bietenholz, and F. G. Rejón-Barrera, New insight into the Berezinskii-Kosterlitz-Thouless phase transition, *J. Phys.: Conf. Ser.* **651**, 012010 (2015).
- [54] L. Wang, Y.-H. Liu, J. Imriška, P. N. Ma, and M. Troyer, Fidelity Susceptibility Made Simple: A Unified Quantum Monte Carlo Approach, *Phys. Rev. X* **5**, 031007 (2015).
- [55] S.-J. Gu and H.-Q. Lin, Scaling dimension of fidelity susceptibility in quantum phase transitions, *Europhys. Lett.* **87**, 10003 (2009), arXiv:0807.3491 [quant-ph].